AD-E400 985

TECHNICAL REPORT ARLCD-TR-83001

ANALYSIS AND SIMULATION OF THE UNWINDING RIBBON, A DELAY ARMING DEVICE

WILLIAM P. DUNN

MARCH 1983

US ARMY ARMAMENT RESEARCH AND DEVELOPMENT COMMAND
LARGE CALIBER
WEAPON SYSTEMS LABORATORY
DOVER, NEW JERSEY

UNCLASSIFIED

SECURITY CLASSIFICATION OF THIS PAGE (When Data Entered)

REPORT DOCUMENTATION PAGE		READ INSTRUCTIONS BEFORE COMPLETING FORM
1. REPORT NUMBER Technical Report ARLCD-TR-83001	2. GOVT ACCESSION NO.	3. RECIPIENT'S CATALOG NUMBER
4. TITLE (and Subtitle) ANALYSIS AND SIMULATION OF THE UNWINDING RIBBON, A DELAY ARMING DEVICE		5. TYPE OF REPORT & PERIOD COVERED 6. PERFORMING ORG. REPORT NUMBER
7. AUTHOR(s) William P. Dunn		8. CONTRACT OR GRANT NUMBER(s)
9. PERFORMING ORGANIZATION NAME AND ADDRESS ARRADCOM, LCWSL Nuclear and Fuze Div (DRDAR-LCN) Dover, NJ 07801		10. PROGRAM ELEMENT, PROJECT, TASK AREA & WORK UNIT NUMBERS
11. CONTROLLING OFFICE NAME AND ADDRESS ARRADCOM, TSD STINFO Div, (DRDAR-TSS) Dover, NJ 07801		12. REPORT DATE March 1983 13. NUMBER OF PAGES 38
14. MONITORING AGENCY NAME & ADDRESS(if different from Controlling Office)		15. SECURITY CLASS. (of this report) UNCLASSIFIED 15a. DECLASSIFICATION/DOWNGRADING SCHEDULE

16. DISTRIBUTION STATEMENT (of this Report)

Approved for public release; distribution unlimited.

17. DISTRIBUTION STATEMENT (of the abstract entered in Block 20, if different from Report)

18. SUPPLEMENTARY NOTES

19. KEY WORDS (Continue on reverse side if necessary and identify by block number)

Delay arming device
Unwinder ribbon
Arming time
Centrifugal force
Arming process
Large deflection bending moment
Spring hub friction

20. ABSTRACT (Continue on reverse side if necessary and identify by block number)

Since the unwinding ribbon has the potential of becoming an inexpensive, simple, and reliable non-horological delay arming device for large caliber munitions (as it has been for small caliber munitions), its equation of motion has been derived for use as a design tool. The solution to this initial value problem has been studied to determine its correlation with experimental results and to determine the sensitivity of the ribbon's behavior to variations in its parameters. The results indicate that the computer simulation of this problem could be used advantageously in designing unwinder ribbon devices.

DD FORM 1 JAN 73 1473 EDITION OF 1 NOV 65 IS OBSOLETE

UNCLASSIFIED

SECURITY CLASSIFICATION OF THIS PAGE (When Data Entered)

CONTENTS

FIGURES

INTRODUCTION

The objective of this work was to provide a mathematical model of the unwinder ribbon capable of predicting the performance of actual hardware using known parameters as input data.

This analysis differs from previous work[1] in that it considers a moment equation derived from the large deflection theory rather than the conventional small deflection formulations. A geometry change in the bridge between the coiled (unstressed) and the recoiled (stressed) material is also considered and is now assumed to be a half-circle rather than a straight line.[2] As a result of the modifications of the mathematical model, fall-off (malfunction) behavior can now be predicted.

UNWINDER DEVICE

The basic components of the unwinder device are shown schematically in figure 1. The spring (A) is wrapped around and fastened at its inner end to the shaft (B). The outer end of the spring is fastened to the outer case (C) at point D. The outer case (C) is fixed to and rotates with the projectile. The axis of the spring and the inner shaft (B) are coincident with the longitudinal axis of the projectile. Upon firing, torsional acceleration causes the spring to wind up tightly. After the torsional acceleration ceases, the centrifugal forces acting on the spring will unwind it. The bending moment in the spring bridge and friction at the hub axis inhibits the unwinding process. During this unwinding process, the inner shaft (B) will rotate relative to the housing. This motion can be used to close a switch, rotate a firing pin in line with a detonator, or initiate some other arming process.

ANALYSIS

Coordinates and Position Vectors (fig. 2)

For a constant angular velocity, ω_o, define (x_o, y_o, z_o), $(x,y,z) \equiv$ inertial frame of reference and body-fixed (imbedded in the hub) coordinate axes, respectively, so that

$$[x(t=0),y(t=0),z(t=0)] = [x_o,y_o,z_o] \tag{1}$$

---

[1] "A New Analysis of the Unwinding Ribbon as a Delayed Arming Device," W. P. Dunn, Proceedings of the 1982 Army Science Conference.

[2] The unwinding ribbon is a spiral-wrapped spring made from flat metal stock closely wound. In the unstressed condition, all coils of the spring are touching.

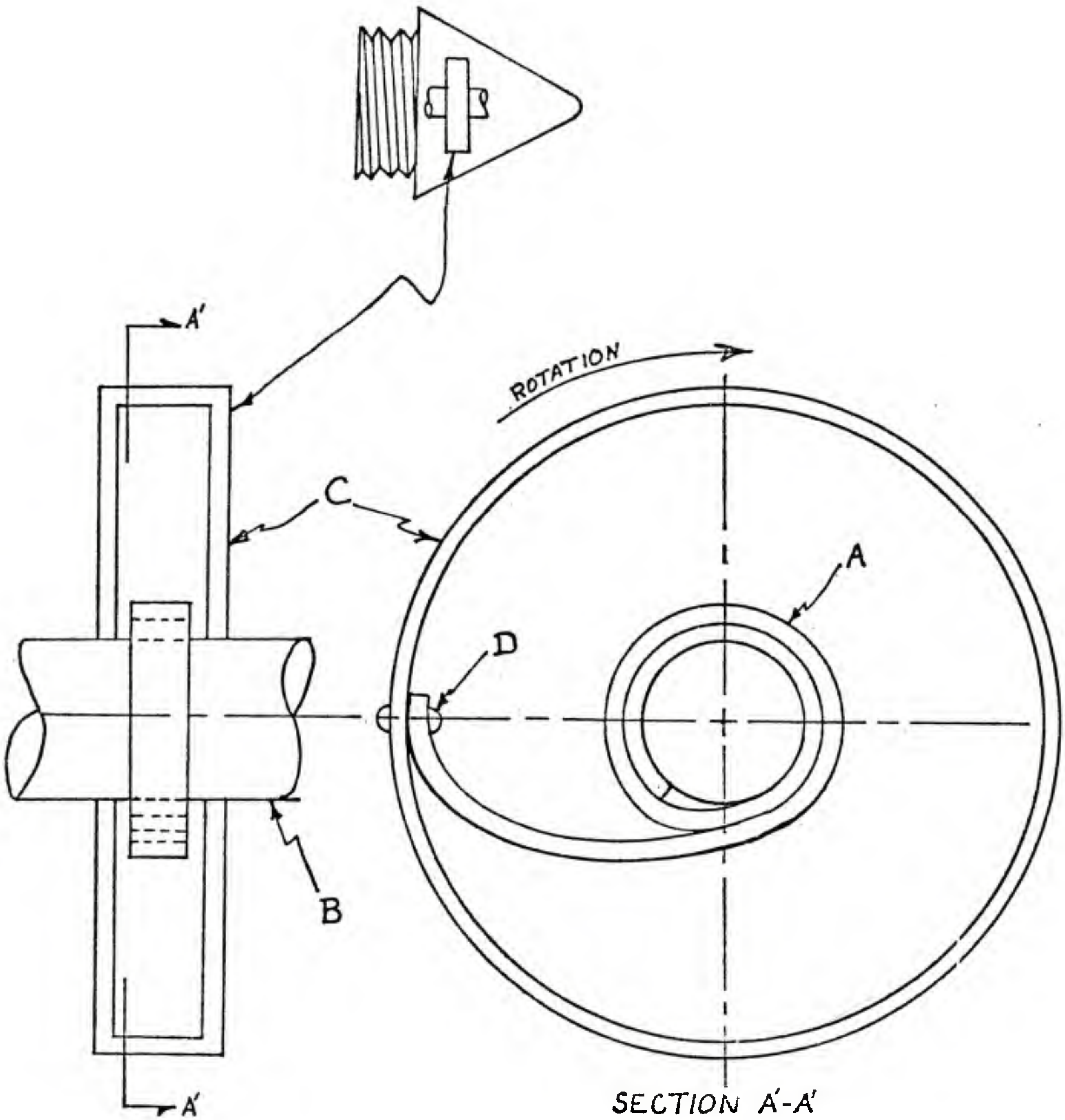

Figure 1. Delayed arming unwinder device

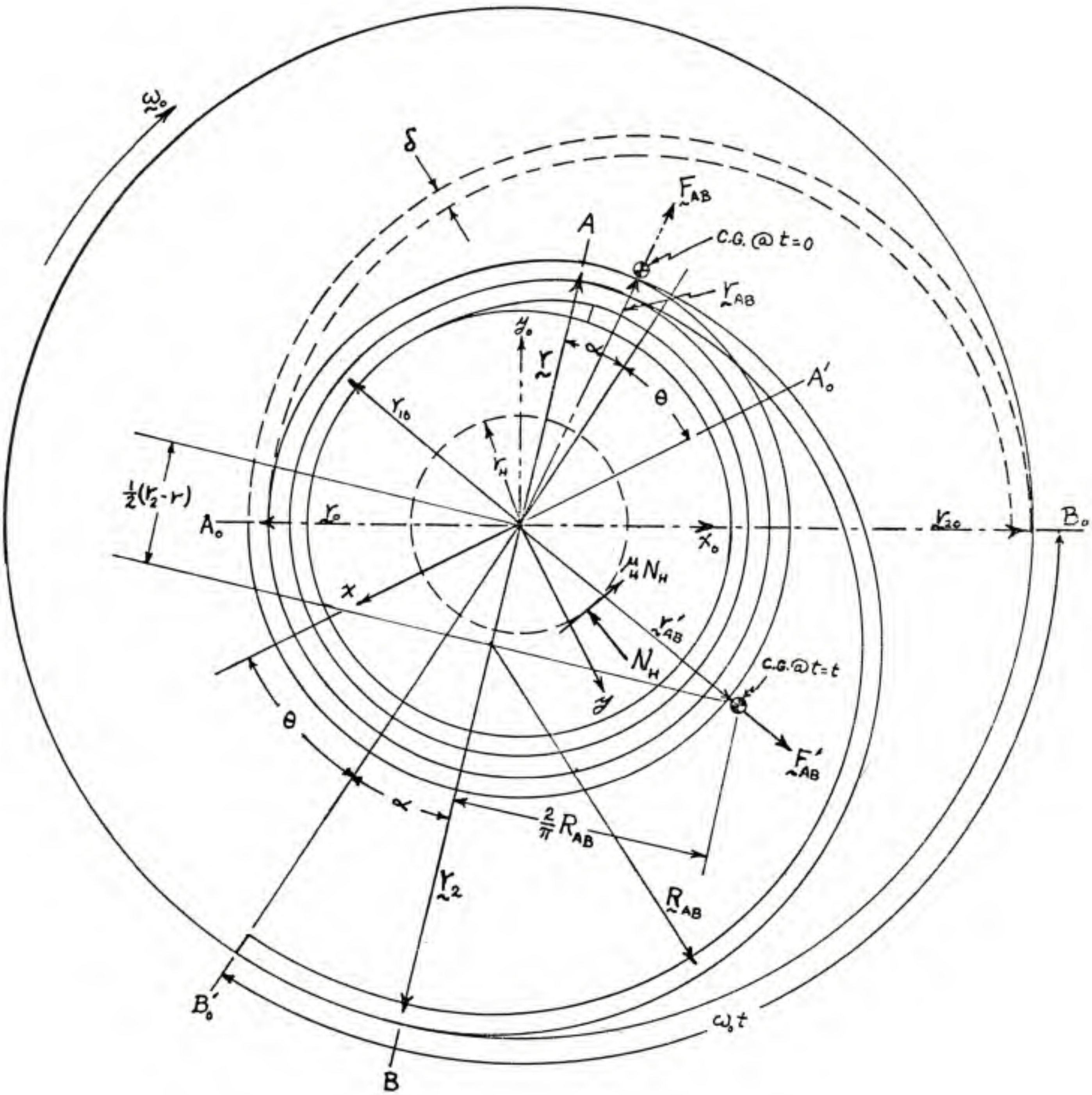

Figure 2. Basic geometry and physical characterization

The unit vectors (i,j,k) of the imbedded coordinate system are related to the inertial reference unit vectors (I,J,K) by

$$\hat{i} = \cos(\omega_o t-\theta)\hat{I} - \sin(\omega_o t-\theta)\hat{J}$$

$$\hat{j} = \sin(\omega_o t-\theta)\hat{I} + \cos(\omega_o t-\theta)\hat{J}$$

$$\hat{k} = \hat{K} \tag{2}$$

where θ is the angle, the hub rotates with respect to the casing and is taken to be negative; t is time and α is the angle characterizing the amount of ribbon material wrapped onto the casing. The position vector to the point at which the center line of the ribbon material just uncoils from the spool, r, and the position vector to the point at which the center line of the ribbon material just begins to coil onto the housing, $\underset{\sim}{r}_2$ are defined by

$$\underset{\sim}{r} = - r[\cos(\alpha-\theta)\hat{i} + \sin(\alpha-\theta)\hat{j}]$$

$$\underset{\sim}{r}_2 = r_2[\cos(\alpha-\theta)\hat{i} + \sin(\alpha-\theta)\hat{j}] \tag{3}$$

where

$$r = r_0-\delta(\alpha-\theta)/2\pi$$

$$r_2 = r_{20}-\delta\alpha/2\pi \tag{4}$$

δ is the ribbon thickness, and r_0, r_{20} are the initial lengths of vectors $\underset{\sim}{r}$ and $\underset{\sim}{r}_2$, respectively

For later use, note that

$$\frac{d\hat{i}}{dt} = -(\omega_o-\dot{\theta})\hat{j} \qquad \frac{d\hat{j}}{dt} = (\omega_o-\dot{\theta})\hat{i} \tag{5}$$

where

$$\dot{\theta} \equiv \frac{d\theta}{dt}$$

The position vector to the center of gravity of the half-circle bridge, $\underset{\sim}{r}'_{AB}$, is defined by

$$\underset{\sim}{r}'_{AB} = \frac{1}{2}(\underset{\sim}{r}_2-\underset{\sim}{r}) + \underset{\sim}{r} + \frac{2}{\pi}\hat{k} \times \frac{1}{2}(\underset{\sim}{r}_2-\underset{\sim}{r}) \tag{6}$$

Substituting equation 3 into equation 6, performing the calculation, and simplifying produces

$$\underset{\sim}{r}'_{AB} = \left[\frac{1}{2} (r_2 - r)\cos(\alpha-\theta) - \frac{1}{\pi} (r_2 + r)\sin(\alpha-\theta) \right]\hat{i}$$

$$+ \left[\frac{1}{2} (r_2 - r)\sin(\alpha-\theta) + \frac{1}{\pi} (r_2 + r)\cos(\alpha-\theta) \right]\hat{j} \qquad (7)$$

To obtain a relationship between α and θ, the length of ribbon material unwrapped from the spool requires an equal length wrapped onto the casing, assuming the bridge material dimensions remain constant. Therefore,

$$\int_o^{(\alpha-\theta)} r\,d(\alpha-\theta) = \int_o^{\alpha} r_2\,d\alpha \qquad (8)$$

Substituting equation 4 into equation 8, integrating, and simplifying yields

$$\alpha = - \frac{r_o \theta + \frac{\delta}{4\pi}\theta^2}{r_{20} - r_o - \frac{\delta}{2\pi}\theta} \qquad (9)$$

Equations of Motion

The vector quantity $\underset{\sim}{F}'_{AB}$ (fig. 2) represents the centrifugal force acting on the half-circle bridge at its center of mass. Again, assuming the mass of the bridge to be constant,

$$\underset{\sim}{F}'_{AB} = -m_{AB} \frac{d^2 \underset{\sim}{r}'_{AB}}{dt^2} \qquad (10)$$

where

$$m_{AB} = \pi \zeta_{SP} b \delta R_{AB} \qquad (11)$$

is the mass of the ribbon bridge, b is the width, ζ_{sp} is the density, and R_{AB} is the radius defined by

$$R_{AB} = \tfrac{1}{2}(r_2 + r) \qquad (12)$$

Since there is only rotational motion, consideration of the forces acting on the free-body of the hub and wound coils (fig. 3) yields

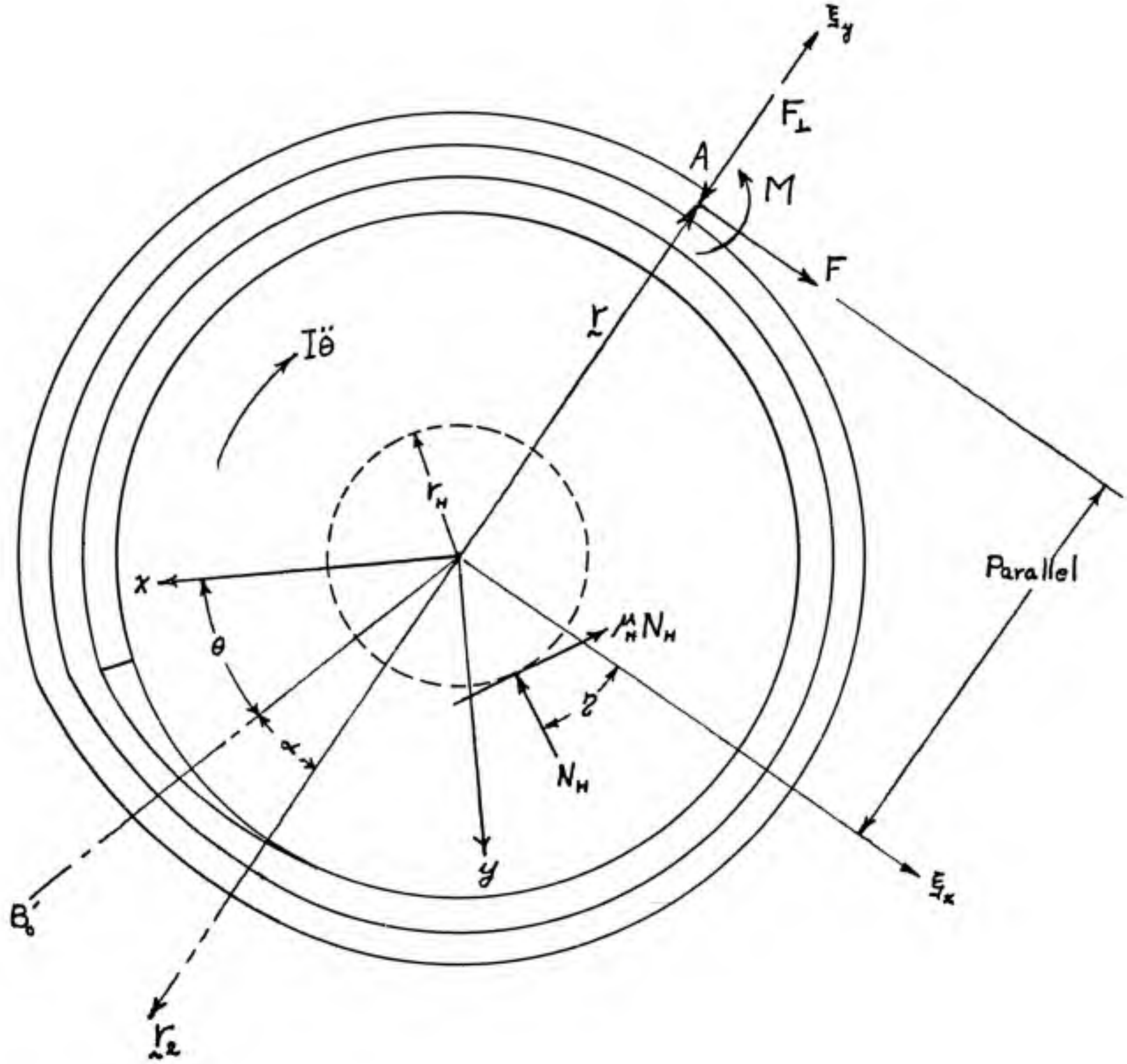

Figure 3. Free-body diagram of the hub and uncoiled ribbon

$$\Sigma F_{\xi x} = 0 \Rightarrow \qquad F = N_H(\cos\eta - \mu_H \sin\eta)$$

$$\Sigma F_{\xi y} = 0 \Rightarrow \qquad F_\perp = N_H(\sin\eta + \mu_H \cos\eta)$$

$$\Sigma M_{\xi z} = \ddot{\theta} I \Rightarrow \qquad I\ddot{\theta} = M - rF + \mu_H r_H N_H \tag{13}$$

where ξ_x, ξ_y are reference coordinates parallel to F and $F_\perp$, respectively. From the first two parts of equation 13

$$\frac{F}{\cos\eta - \mu_H \sin\eta} = \frac{F_\perp}{\sin\eta - \mu_H \cos\eta}$$

or

$$\sin\eta = \left(\frac{F_\perp - \mu_H F}{F + \mu_H F_\perp}\right) \cos\eta \tag{14}$$

Using $\sin^2\eta + \cos^2\eta = 1$, the square of equation 14 produces

$$\sin\eta = \frac{F_\perp - \mu_H F}{\sqrt{(1 + \mu_H^2)(F^2 + F_\perp^2)}} \qquad \cos\eta = \frac{F + \mu_H F_\perp}{\sqrt{(1 + \mu_H^2)(F^2 + F_\perp^2)}} \tag{15}$$

Substituting the first part of equation 13 into the last part produces

$$I\ddot{\theta} = M - \left(r - \frac{\mu_H r_H}{\cos\eta - \mu_H \sin\eta}\right)F \tag{16}$$

Substituting equation 15 into equation 16 then yields

$$I\ddot{\theta} - M + rF = \mu_H r_H \sqrt{\frac{F^2 + F_\perp^2}{1 + \mu_H^2}} \tag{17}$$

where M is the bending moment in the ribbon (to be derived later), N_H is the normal force of the hub on the hub casing, and $F_\perp$ is a component of $\underset{\sim}{F}'_{AB}$. The term r_H denotes the radius of the spool hub; μ_H denotes the friction coefficient between the hub and hub casing; I is the mass moment of inertia of the hub plus wound coils about the coordinate origin; $\ddot{\theta} \equiv \frac{d^2\theta}{dt^2}$ is the angular acceleration of the hub, and F is a scalar component of $\underset{\sim}{F}'_{AB}$ which is perpendicular to $F_\perp$ and tangent to the coils at A. These terms (F, $F_\perp$) are obtained explicitly by using the relations

$$F = \underset{\sim}{F}'_{AB} \cdot (\hat{k} \times \underset{\sim}{r}_{2}/r_2)$$

$$F_{\perp} = \underset{\sim}{F}'_{AB} \cdot \underset{\sim}{r}_{2}/r_2 \tag{18}$$

Return to equation 7 and define R_1 and R_2 so that

$$\underset{\sim}{r}'_{AB} = R_1\hat{i} + R_2\hat{j} \tag{19}$$

where

$$R_1 \equiv \frac{1}{2}(r_2 - r)\cos(\alpha-\theta) - \frac{1}{\pi}(r_2 + r)\sin(\alpha-\theta)$$

$$R_2 \equiv \frac{1}{2}(r_2 - r)\sin(\alpha-\theta) + \frac{1}{\pi}(r_2 + r)\cos(\alpha-\theta) \tag{20}$$

Taking the time derivatives of equation 20 results in

$$\dot{R}_1 = (\dot{\alpha}-\dot{\theta})R_2$$

$$\dot{R}_2 = (\dot{\alpha}-\dot{\theta})R_1 \tag{21}$$

where $\dot{r}$, $\dot{r}_2$ terms are neglected compared to $\dot{\alpha}$, $\dot{\theta}$ terms. One more time derivative of equation 21 produces

$$\ddot{R}_1 = -(\ddot{\alpha}-\ddot{\theta})R_2 - (\dot{\alpha}-\dot{\theta})^2 R_1$$

$$\ddot{R}_2 = (\ddot{\alpha}-\ddot{\theta})R_1 - (\dot{\alpha}-\dot{\theta})^2 R_2 \tag{22}$$

Therefore, using equations 5 and 21, equation 19 yields

$$\dot{\underset{\sim}{r}}'_{AB} = (\omega_o - \dot{\alpha})(R_2\hat{i} - R_1\hat{j}) \tag{23}$$

The time derivative of equation 23 then becomes

$$\ddot{\underset{\sim}{r}}'_{AB} = -\{[\ddot{\alpha}R_2 + (\omega_o - \dot{\alpha})^2 R_1]\hat{i} + [-\ddot{\alpha}R_1 + (\omega_o - \dot{\alpha})^2 R_2]\hat{j}\} \tag{24}$$

where, from equation 9,

$$\dot{\alpha} = -\frac{(r_{20} - r_o)\left(r_o + \frac{\delta\theta}{2\pi}\right) - \frac{1}{8}\left(\frac{\delta\theta}{\pi}\right)^2}{\left(r_{20} - r_o \;\; \delta\theta/2\pi\right)^2}\,\dot{\theta}$$

$$\ddot{\alpha} = \frac{\dot{\alpha}}{\dot{\theta}}\,\ddot{\theta} - \frac{\delta\left(r_{20}^{\;2} - r_o^{\;2}\right)}{2\pi\left(r_{20} - r_o - \delta\theta/2\pi\right)^3}\,\dot{\theta}^2 \tag{25}$$

Substituting equation 24 into equation 10, substituting this result into equation 18, and simplifying produces

$$F = \frac{m_{AB}}{2\pi}\left[\pi(r_2-r)\ddot{\alpha} - 2(r_2+r)(\omega_o-\dot{\alpha})^2\right]$$

$$F_\perp = \frac{m_{AB}}{2\pi}\left[2(r_2+r)\ddot{\alpha} + \pi(r_2-r)(\omega_o-\dot{\alpha})^2\right] \tag{26}$$

Defining

$$G_1 \equiv \frac{(r_{20} - r_o)(r_o + \delta\theta/2\pi) - \frac{1}{8}(\delta\theta/\pi)^2}{(r_{20} - r_o - \delta\theta/2\pi)^2}$$

$$G_2 \equiv \frac{\delta\left(r_{20}^{\ 2} - r_o^{\ 2}\right)}{2\pi(r_{20} - r_o - \delta\theta/2\pi)^3} \tag{27}$$

equation 25 can be written

$$\dot{\alpha} = -G_1\dot{\theta} \qquad \ddot{\alpha} = -G_1\ddot{\theta} - G_2\dot{\theta}^2 \tag{28}$$

The mass moment of inertia, I, of the hub plus wound ribbon can be written as

$$I = I_H + \frac{1}{2}\pi\,\zeta_{SP}b\left(r^4 - r_{10}^{\ 4}\right) \tag{29}$$

where I_H is the measured mass moment of inertia of the hub.

Bending Moment in the Ribbon Bridge

It is assumed that the bending moment (produced by a ribbon element of radius r in the unstressed state, deformed to a radius of curvature r_2 in the stressed state) is equivalent to the bending moment in a quarter circle, cantilever beam going from a radius r in the undeformed state to a radius r_2 in the deformed state. This is represented in figure 4.

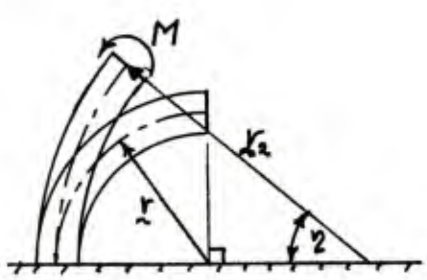

Figure 4. Large deflection of quarter circle-cantilever beam

Assuming the beam centerline to be the neutral axis, the length of the neutral fiber in the deformed and undeformed configurations must be equal. Therefore, from figure 4

$$\pi r/2 = \eta r_2 \Rightarrow \qquad \eta = \frac{\pi r}{2r_2} \tag{30}$$

The bending moment due to fiber stress is defined by

$$M = b\int_{-\delta/2}^{\delta/2} y\sigma dy \tag{31}$$

where the integration is over the ribbon thickness and σ, the stress in the fibers, is related to the fiber strains, ε, by

$$\sigma = E\varepsilon \tag{32}$$

Where E is the elastic modulus and ε, the strain, is defined by

$$\varepsilon = \frac{\Delta L}{L} \tag{33}$$

Here L is the original fiber length and ΔL is the change in fiber length due to deformation. They are defined by

$$L = \frac{\pi}{2}(r+y) \qquad \Delta L = \frac{\pi}{2}(r+y) - \eta(r_2+y) \tag{34}$$

Substitute equation 34 into 33 and obtain from equation 32

$$\sigma = E\,(1-r/r_2)\,\frac{y}{r+y} \tag{35}$$

Then substituting equation 35 into equation 31, integrating, and simplifying results in

$$M = bEr\left(1 - \frac{r}{r_2}\right)\left[r\ln\left(\frac{2r+\delta}{2r-\delta}\right) - \delta\right] \tag{36}$$

Computational Form of the Equations of Motion

Having the necessary ingredients to evaluate equation 17, the various terms will be redefined for convenient handling and computational facilitation. Sub-

stituting equations 28 into 26 and substituting these results into equation 17, solving for $\ddot{\theta}$, and simplifying produces

$$\ddot{\theta} = \frac{1}{2A_6}\left(A_7 + \sqrt{A_7^2 - 4A_6A_8}\right) \tag{37}$$

where

$$A_8 = A_3 - \frac{\mu_H^2 r_H^2}{1 + \mu_H^2} A_5 \qquad A_6 = A_1 - \frac{(\mu_H r_H G_1)^2}{1 + \mu_H^2} A_4$$

$$A_7 = A_2 + \frac{2\,\mu_H^2 r_H^2 G_1 G_2}{1 + \mu_H^2} A_4 \dot{\theta}^2 \qquad A_5 = A_4\left[G_2^2\,\dot{\theta}^4 + (\omega_o + G_1\dot{\theta})^4\right]$$

$$A_4 = \left(\frac{m_{AB}}{2\pi}\right)^2 \left[\pi^2 (r_2 - r)^2 + 4\,(r_2 + r)^2\right] \tag{38}$$

$$A_3 = \left\{M - \frac{r m_{AB}}{2\pi}\left[\pi (r_2 - r) G_2 \dot{\theta}^2 + 2(r_2 + r)(\omega_o + G_1\dot{\theta})^2\right]\right\}$$

$$A_2 = \left\{M - \frac{1}{\pi} m_{AB} r (r_2 + r)(\omega_o + G_1\dot{\theta})^2 - \frac{1}{2} m_{AB} r (r_2 - r) G_2 \dot{\theta}^2\right\} X \left\{2I + m_{AB} r (r_2 - r) G_1\right\}$$

$$A_1 = \left[I + \frac{1}{2} r (r_2 - r) m_{AB} G_1\right]^2$$

Equation 37 is the defining equation of motion of the wound coils of the unwinder plus the hub. The particular solution is obtained from the initial conditions

$$\theta(t = 0) = 0 \qquad \dot{\theta}\,(t = 0) = 0 \tag{39}$$

Supplemental Computations

To complete the computations, the values of r_o and α_{MAX}, θ_{MAX} (the angles denoting a completely unwound ribbon) must be determined. The value r takes when the ribbon is completely unwound (eq 3) is r_{10} and therefore

$$r_{10} = r_o - \frac{\delta}{2\pi}\left(\delta_{MAX} - \theta_{MAX}\right) \tag{40}$$

Also, for a given ribbon length, L,

$$L = \int_{0}^{\alpha_{MAX} - \theta_{MAX}} r d(\alpha-\theta) \quad = r_o(\alpha_{MAX} - \theta_{MAX}) - \frac{\delta}{4\pi}(\alpha_{MAX} - \theta_{MAX})^2 \tag{41}$$

Solving for $\alpha_{MAX} - \theta_{MAX}$ from equation 40; substituting the result into equation 41, and solving for r_o

$$r_o = \left(r_{10}{}^2 + \frac{\delta L}{\pi}\right)^{1/2} \tag{42}$$

The maximum wrapping angle, α_{MAX}, is obtained by noting that

$$L = \int_{0}^{\alpha_{MAX}} r_2 d\alpha = r_{20}\alpha_{MAX} - \frac{\delta}{4\pi}\alpha_{MAX}^2 \tag{43}$$

Solving equation 43 for α_{MAX} results in

$$\alpha_{MAX} = \frac{2\pi r_{20}}{\delta}\left(1 - \sqrt{1 - \delta L/r_{20}{}^2}\right) \tag{44}$$

Substituting equations 42 and 44 into equation 40 gives the radians the hub rotates relative to the fuze casing as

$$\theta_{MAX} = \frac{2\pi}{\delta}\left\{r_{20}\left(1 - \sqrt{1 - \delta L/\pi r_{20}{}^2}\right) + r_{10}\left(1 - \sqrt{1 - \delta L/\pi r_{10}{}^2}\right)\right\} \tag{45}$$

RESULTS OF COMPUTER SIMULATION

The logic and equation of motion for the arming time of the unwinding ribbon wave was programmed for the CDC 6600 computer using FORTRAN. A fourth order Runge-Kutta routine was used to solve the differential equation 37. The basic program and sample input-output for spring 1 is contained in the appendix.

The results of this analysis compared to the experimental findings of T. B. Alfriend[3] are shown in figures 5 through 11. The analysis illustrated in figures 5 and 11 shows more resistance to motion than indicated by experiment. In particular, where none of the ribbons completely unwind (fig. 5), the analysis is conservative in that fewer coils are predicted to unwind from the coil than actually do. This error appears to be less as the angular speed increases; therefore, the inertial centrifugal force overwhelms both the bending movement in the bridge and frictional resistance.

The analysis in figures 6 through 10 shows less resistance to motion than indicated by experiment although figures 6, 10, and 11 show qualitatively good results.

A parametric study was made to determine the effect of the various input quantities on the results of the analysis. The effects of varying ω_o, r_{10}/r_{20}, δ, and μ_H are shown in figures 12 through 15. It appears that the arming time for a given configuration is most sensitive to the ratio r_{10}/r_{20} and therefore the ratio r_{10}/r_{20} could be a critical factor in the design of the unwinder ribbon.

CONCLUSIONS AND RECOMMENDATIONS

Since good correlation between theoretical and experimental results has been obtained (quantitatively for 13 of the 20 experiments and qualitatively for the remaining 7 experiments), this analysis offers the engineer a potentially powerful design tool for the development of winding ribbons.

As adjustment of the parameters ω_o, r_{10}/r_{20}, δ, and μ_H can affect the correlation of analytic and experimental results, it is recommended that new tests be conducted with careful measurements of the actual dimensions, angular speeds, and friction coefficients.

Improved accuracy of the analysis may be obtained by including both the effect of $\dot{r}$, $\dot{r}_2$, and the change in mass of the bridge, i.e.,

$$\underset{\sim}{F}'_{AB} = -\frac{d}{dt}\left(m_{AB}\, \dot{\underset{\sim}{r}}'_{AB}\right) = -\dot{m}_{AB}\, \dot{\underset{\sim}{r}}'_{AB} - m_{AB}\, \ddot{\underset{\sim}{r}}'_{AB}$$

This, however, would involve considerable mathematical complexity and should not be considered unless the comparison of theoretical and new experimental results makes it necessary. The accuracy of the assumption that the ribbon coiled on the hub is in a stress-free state should be verified.

---

3 "Study of Wrapped Springs for Application to a Delayed Arming Device," T. B. Alfriend, Summary Report ER-1404, Aircraft Armaments, Inc., 1958.

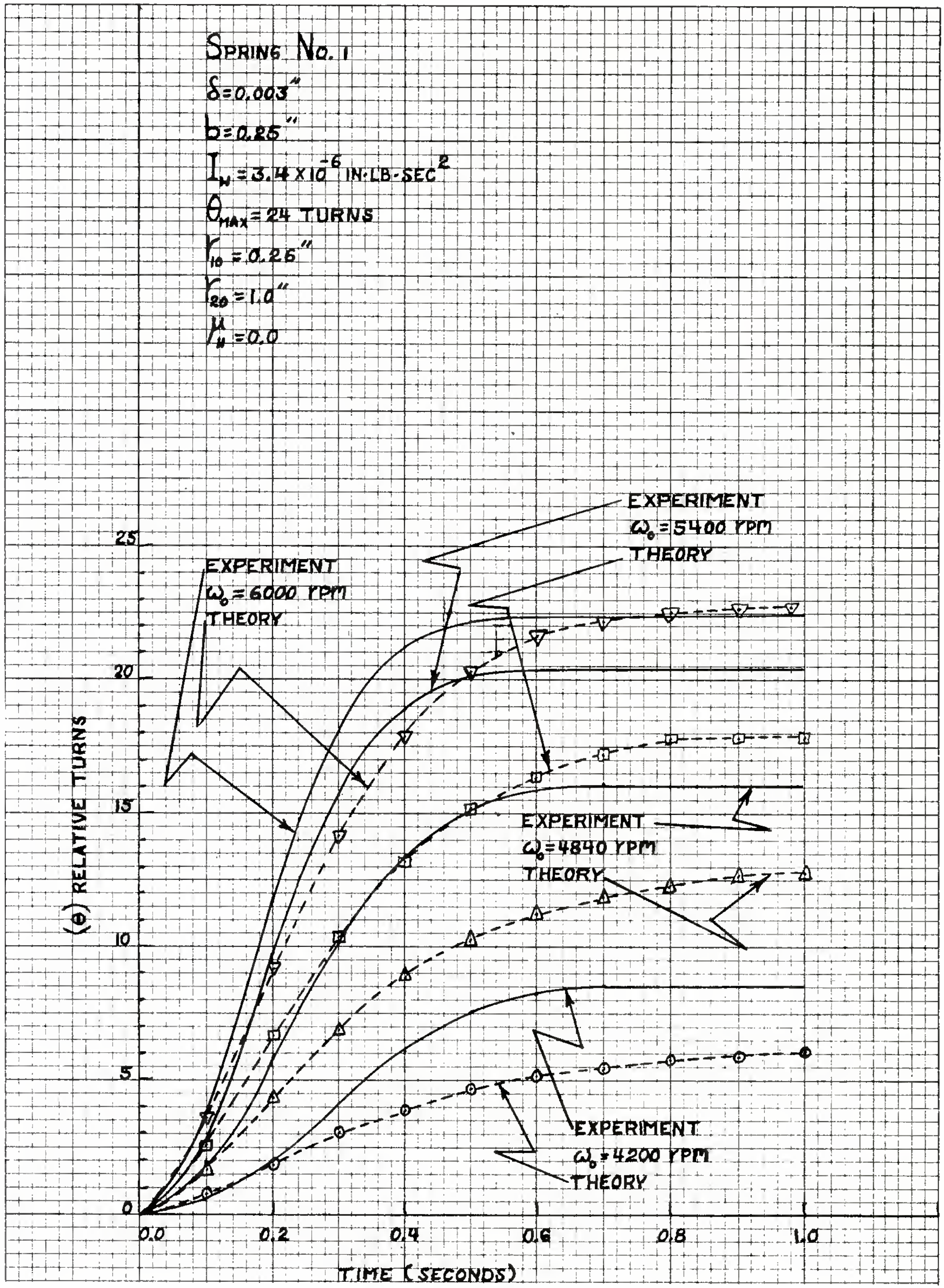

Figure 5. Spring 1, relative turns versus time

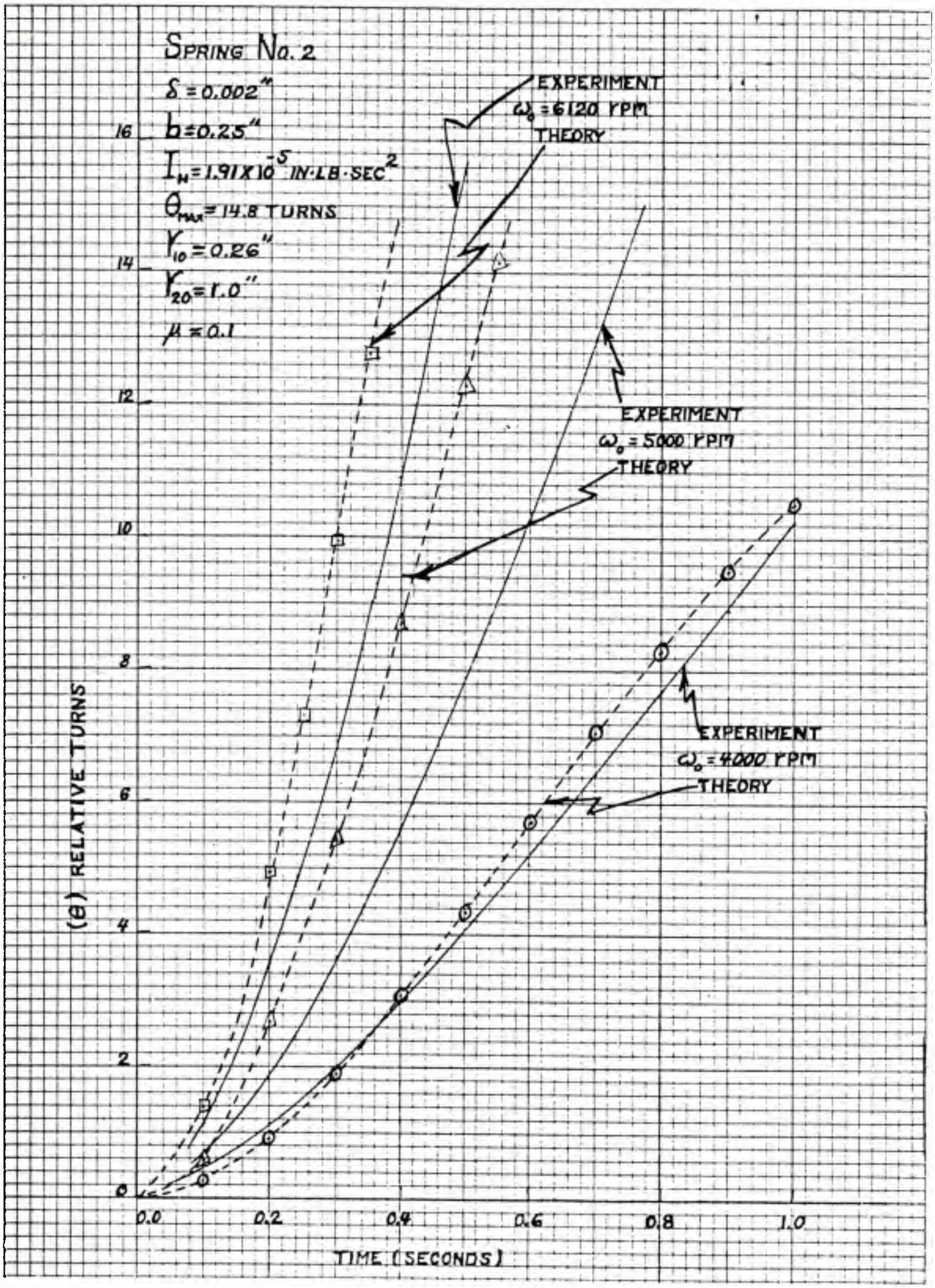

Figure 6. Spring 2, relative turns versus time

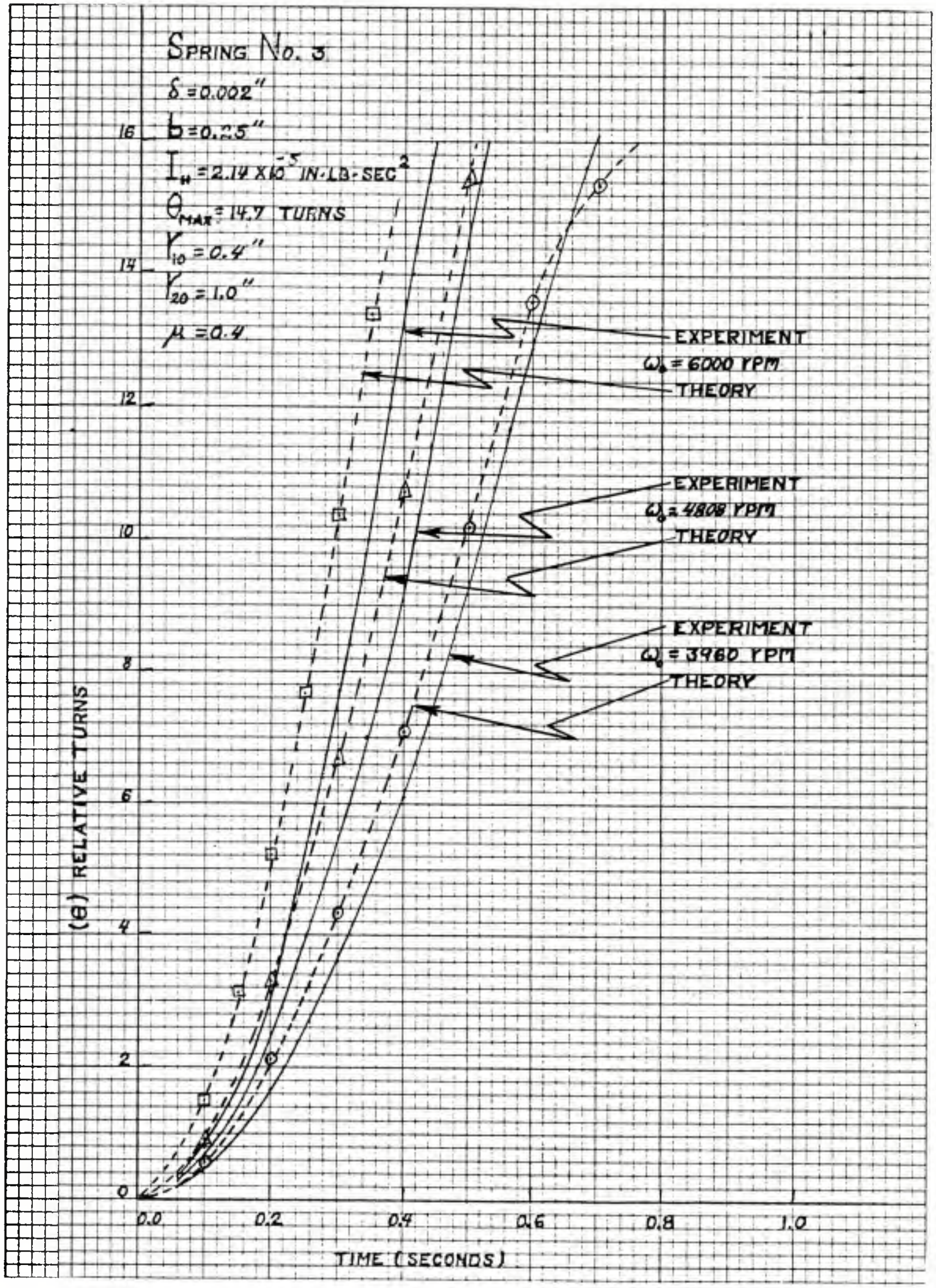

Figure 7. Spring 3, relative turns versus time

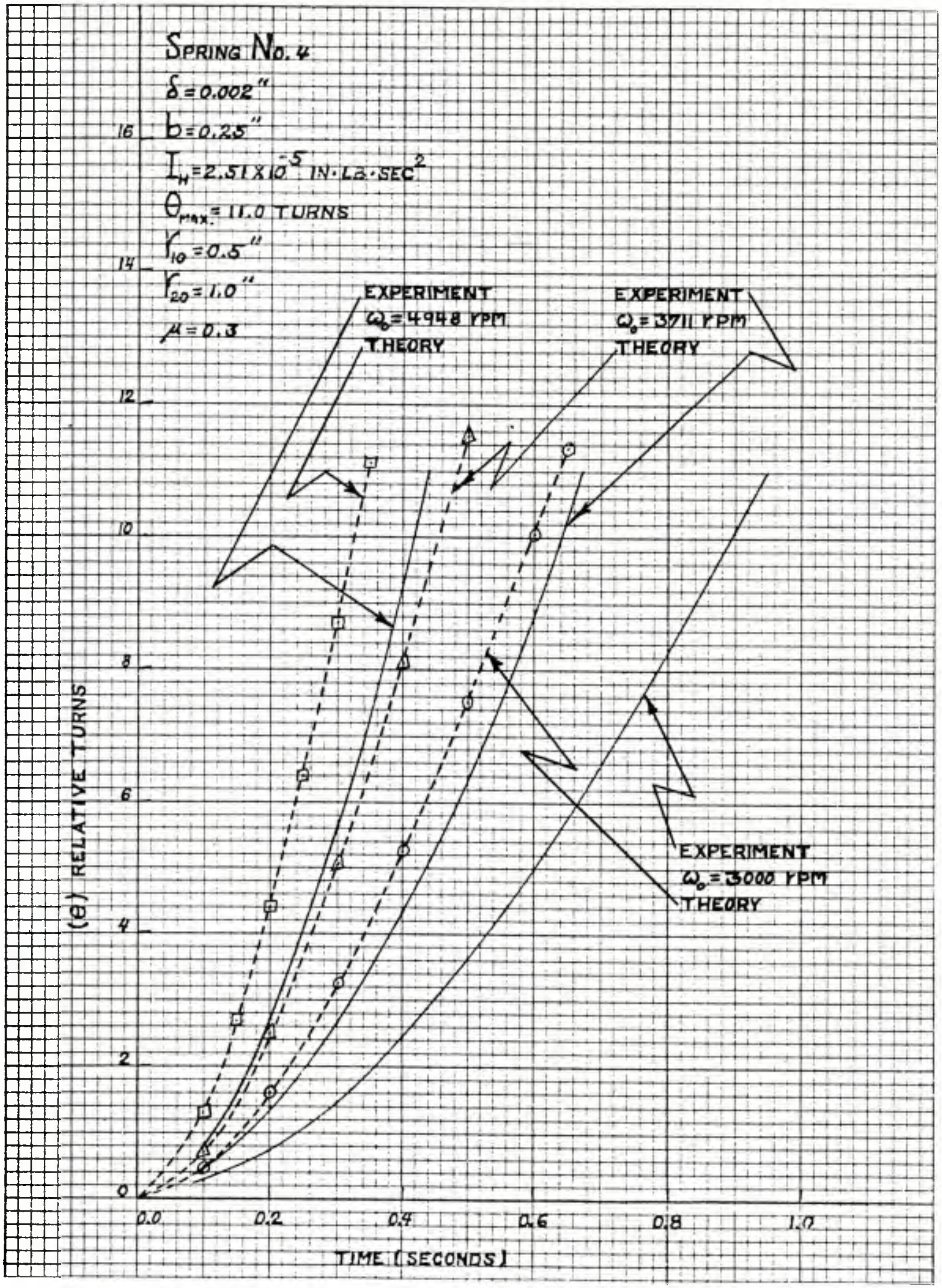

Figure 8. Spring 4, relative turns versus time

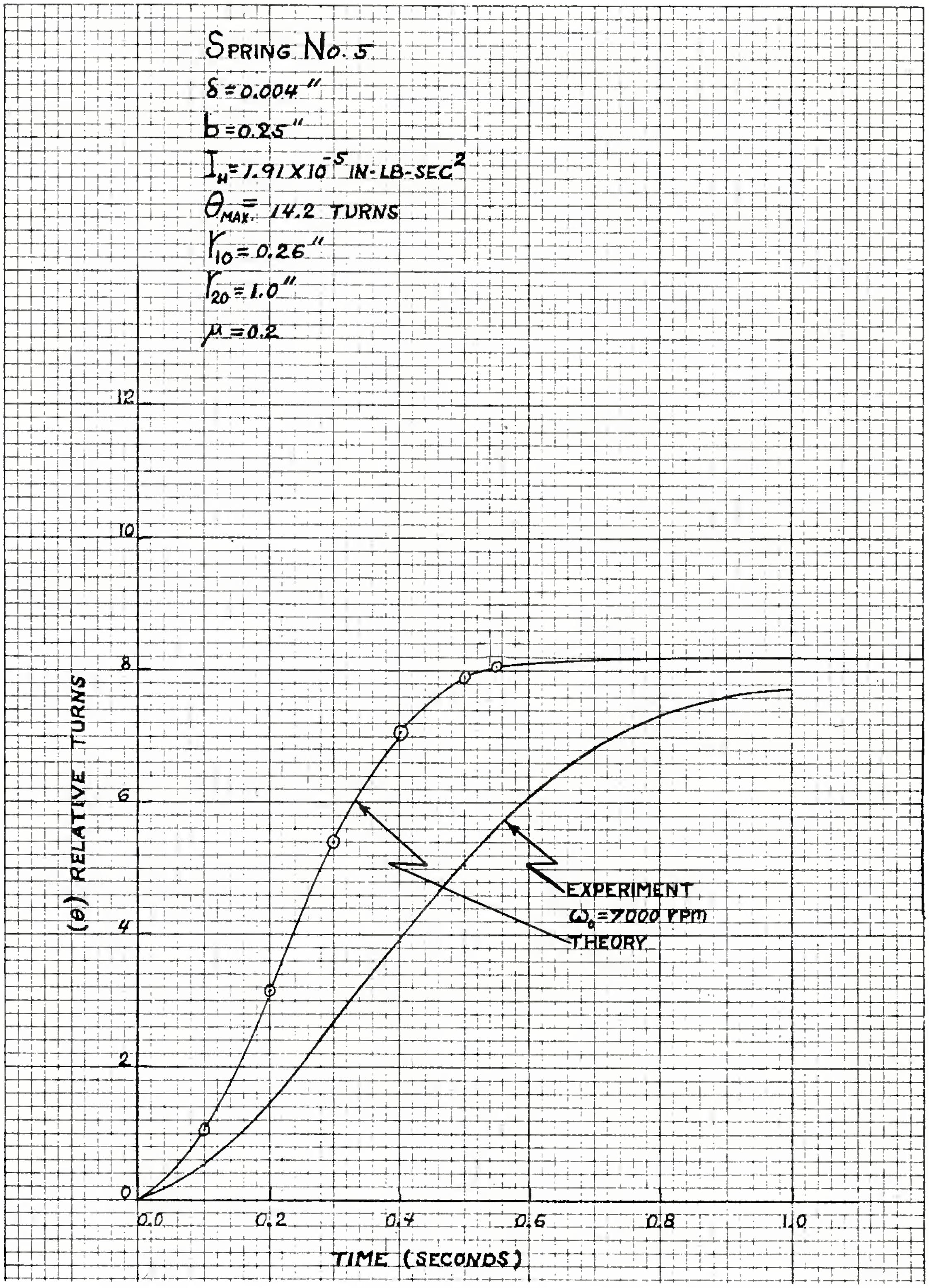

Figure 9. Spring 5, relative turns versus time

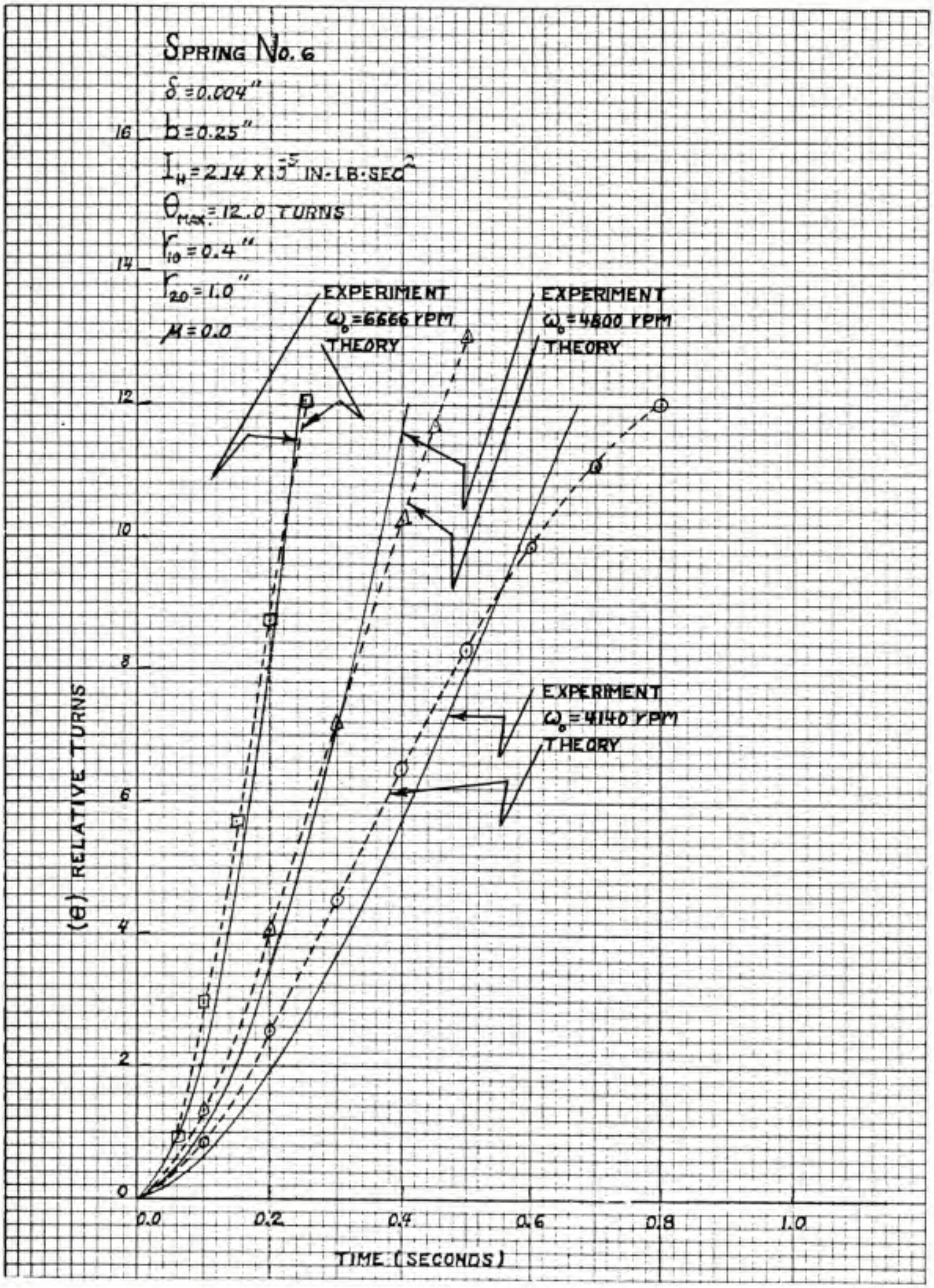

Figure 10. Spring 6, relative turns versus time

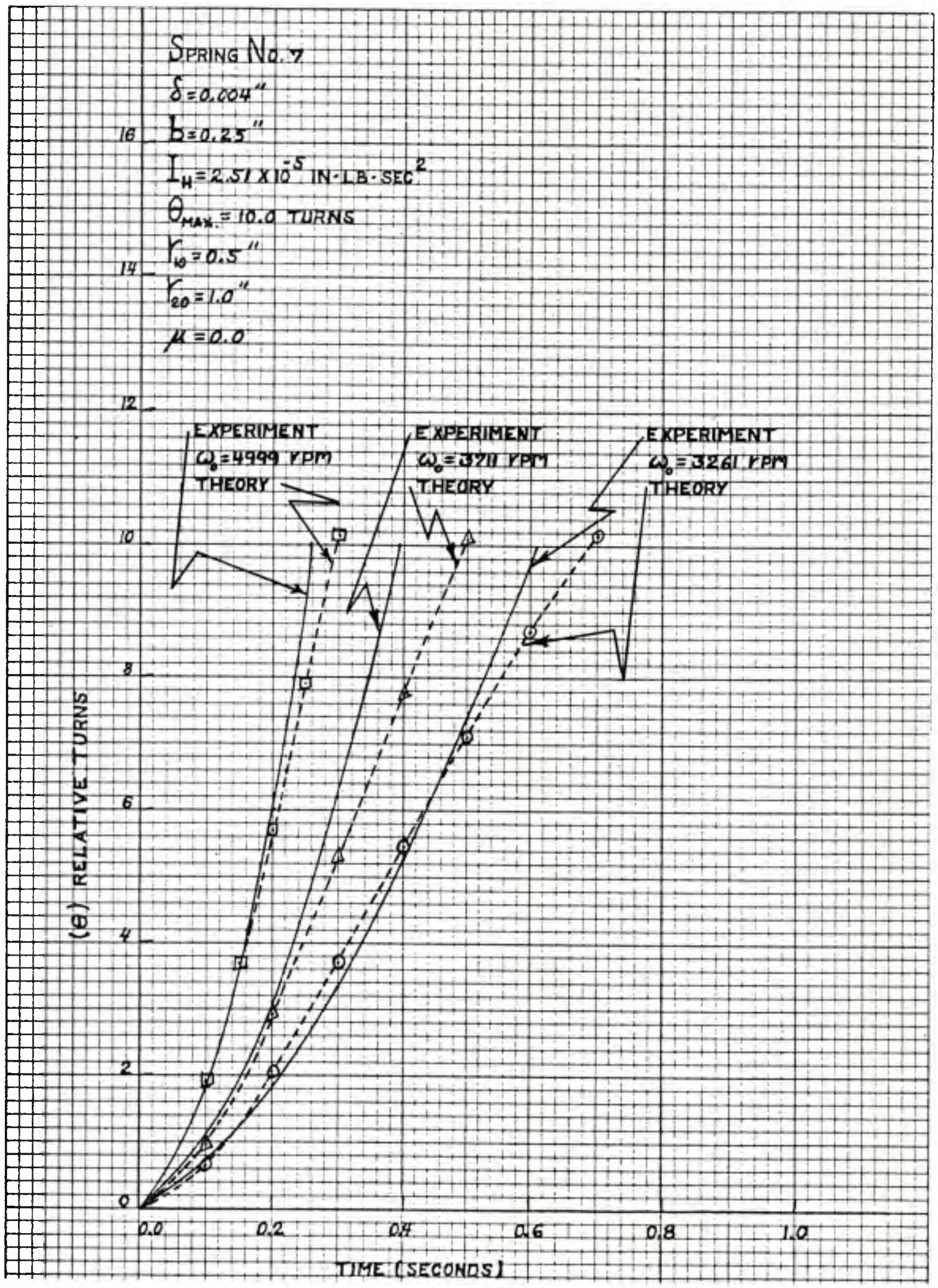

Figure 11. Spring 7, relative turns versus time

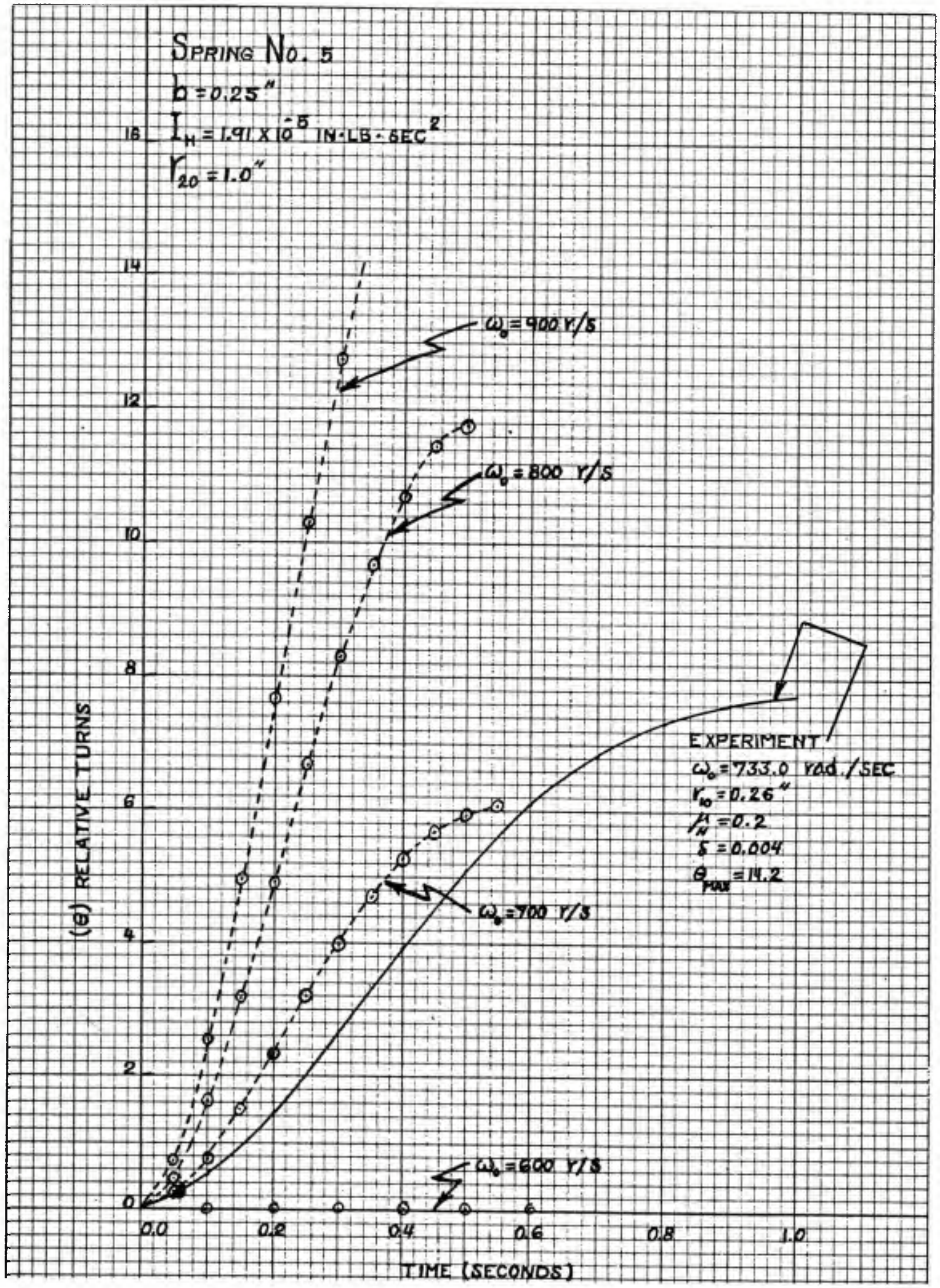

Figure 12. Spring 1, effect of spin-rate (ω_o) on arming

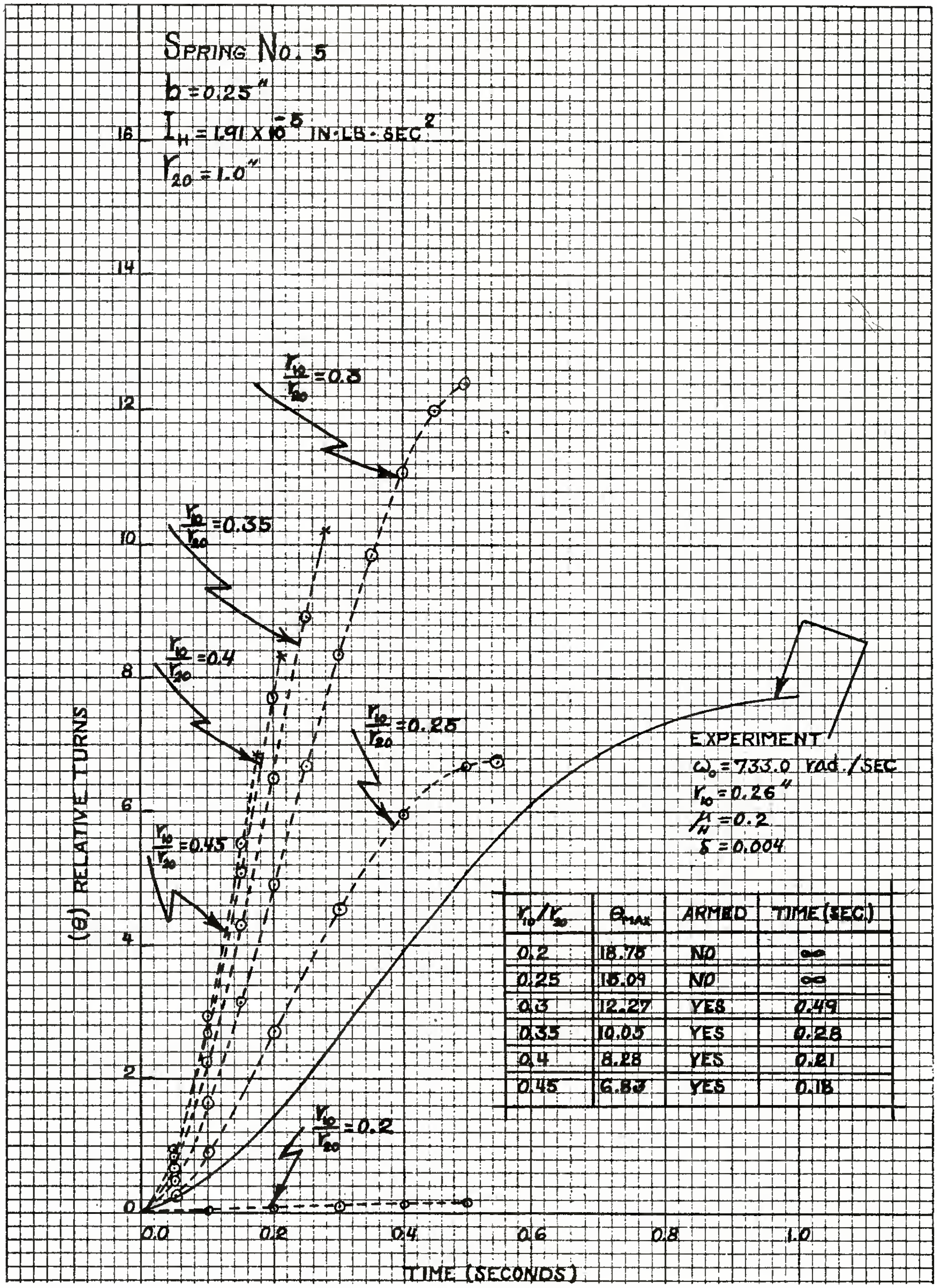

r_{10}/r_{20}	θ_{MAX}	ARMED	TIME (SEC)
0.2	18.75	NO	∞
0.25	15.09	NO	∞
0.3	12.27	YES	0.49
0.35	10.05	YES	0.28
0.4	8.28	YES	0.21
0.45	6.83	YES	0.18

Figure 13. Spring 1, effect of r_{10}/r_{20} on arming and arming time

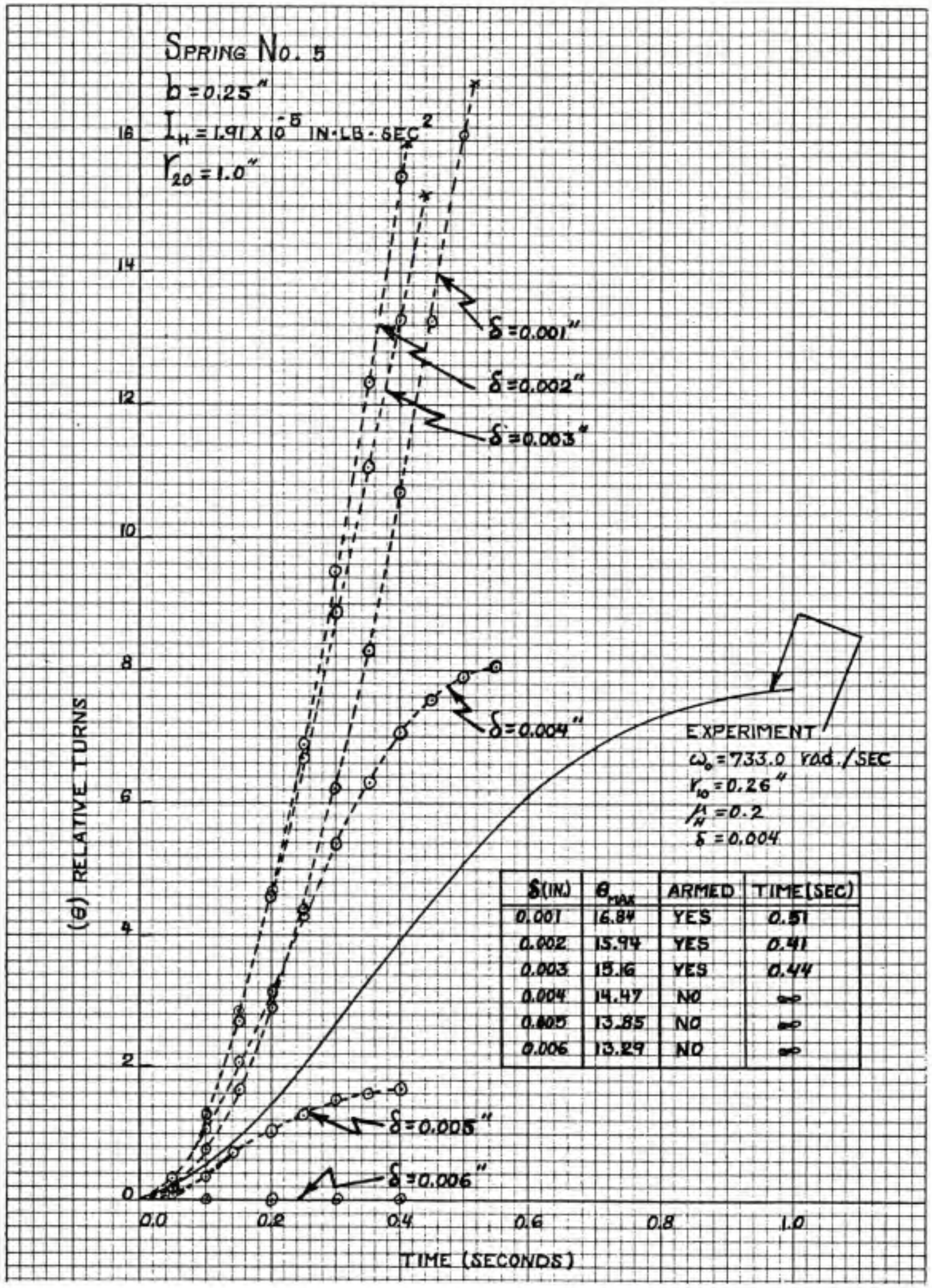

Figure 14. Spring 1, effect of ribbon thickness on arming

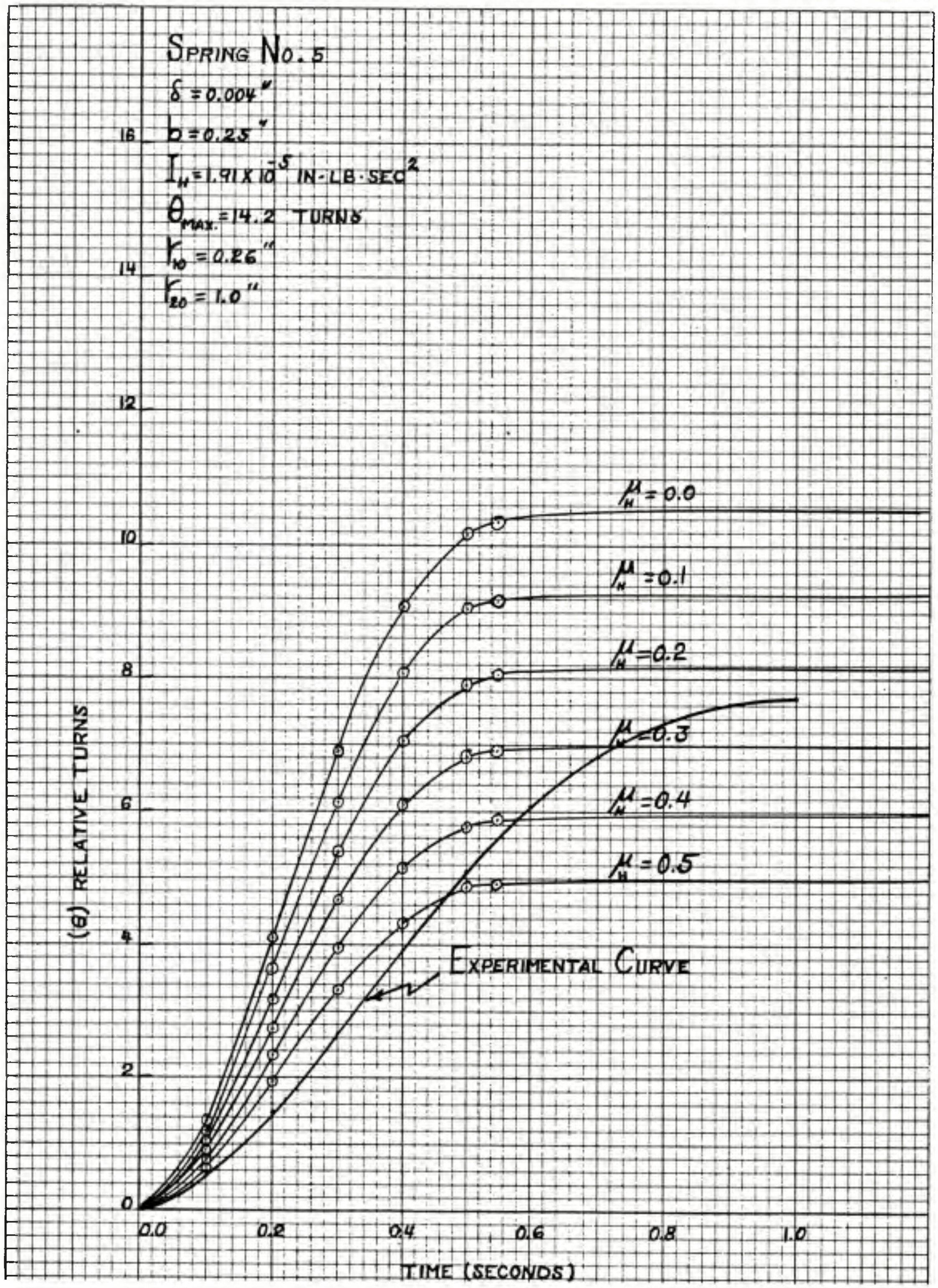

Figure 15. Spring 1, effect of hub friction (μ_H) on arming

APPENDIX

COMPUTER PROGRAM AND SAMPLE INPUT-OUTPUT DATA

```
      PROGRAM SPINNER(INPUT,OUTPUT,TAPE5=INPUT,TAPE6=OUTPUT)
C
C     ?????????????????????????????????????????????????????????????????
C     THIS PROGRAM COMPUTES A MODIFIED ALFRIEND RELATION TO BE COUPLED
C     WITH EXPERIMENTAL TECHNOLOGY FOR ENGINEERING DESIGN OF UNWINDER
C     FUZES.
C     '''''''''''''''''''''''''''''''''''''''''''''''''''''''''''''''''
C
      COMMON DELTA,B,R10,R20,R0,E,RHOSP,RHOSH,M,L,OMO,RC,ALPHA,PI,I,
     1TURNMAX,MU,RH,RCM,IH
      REAL M,L,I,MU,MAB,IH
      DIMENSION THETA(2),DTHETA(2),PRMT(5),AUX(8,2)
      EXTERNAL FCT,OUTP
      NDIM=2
      PI=3.14159
      READ(5,1)DELTA,B,R10,R20,E,RHOSP,RHOSH,L,OMO,MU,IH
    1 FORMAT(4(F10.4/),3(E10.2/)3(F10.4/),E10.2)
      WRITE(6,2)DELTA,B,R10,R20,E,RHOSP,RHOSH,L,OMO,MU,IH
    2 FORMAT(*1DELTA=*,F5.3/*0B=*,F5.3/*0R10=*,F4.2/*0R20=*,F4.2/*0E=*,
     1E10.2/*0RHOSP=*,E10.2/*0RHOSH=*,E10.2/*0L=*,F5.1/*0OMO=*,F6.1/*0
     2MU=*,F6.4/*0IH=*,E10.2///)
      R0=SQRT(DELTA*L/PI+R10**2)
      ALMAX=2.*PI*R20*(1.-SQRT(1.-DELTA*L/(PI*R20**2)))/DELTA
      THETMAX=2.*PI*(R20*(1.-SQRT(1.-DELTA*L/(PI*R20**2)))+R10*(1.-
     1SQRT(1.+DELTA*L/(PI*R10**2))))/DELTA
      TURNMAX=-THETMAX/(2.*PI)
      RH=R10/2.
      RC=SQRT(R20**2-R0**2)
      PRMT(1)=0.
      PRMT(2)=1.
      PRMT(3)=.001
      PRMT(4)=.1
      THETA(1)=.0
      THETA(2)=.0
      DTHETA(1)=.5
      DTHETA(2)=.5
      CALL RKGS(PRMT,THETA,DTHETA,NDIM,IHLF,FCT,OUTP,AUX)
      STOP
      END
```

```
      SUBROUTINE FCT (TIME,THETA,DTHETA)
      DIMENSION THETA(2),DTHETA(2)
      COMMON DELTA,B,R10,R20,RO,E,RHOSP,RHOSH,M,L,OMO,RC,ALPHA,PI,I,
     1TURNMAX,MU,RH,RCM,IH
      REAL M,L,I,MU,MAB,IH
      DTHETA(1)=THETA(2)
      ALPHA=-(RO+DELTA*THETA(1)/(4.*PI))*THETA(1)/(R20-RO-DELTA*THETA(1)
     1/(2.*PI))
      R=RO-DELTA*(ALPHA-THETA(1))/(2.*PI)
      I=IH+PI*RHOSP*B*(R**4-R10**4)/2.
      R2=R20-DELTA*ABS(ALPHA)/(2.*PI)
      RAB=(R2+R)/2.
      M=E*B*R*(1.-R/R2)*(-DELTA+R*ALOG((2.*R+DELTA)/(2.*R-DELTA)))
      MAB=PI*RHOSP*RAB*B*DELTA
      G1=((R20-RO)*(RO+DELTA*THETA(1)/(2.*PI))-(DELTA*THETA(1)/(2.*PI))
     1**2/2.)/(R20-RO-DELTA*THETA(1)/(2.*PI))**2
      G2=DELTA*(R20**2-RO**2)/(2.*PI*(R20-RO-DELTA*THETA(1)/(2.*PI))**3)
      A1=(I+R*(R2-R)*MAB*G1/2.)**2
      A2=(M-MAB*R*(R2+R)*(OMO+G1*THETA(2))**2/PI-MAB*R*(R2-R)*G2*
     1THETA(2)**2/2.)*(2.*I+MAB*R*(R2-R)*G1)
      A3=(M-R*MAB*(PI*(R2-R)*G2*THETA(2)**2+2.*(R2+R)*(OMO+G1*THETA(2))
     1**2)/(2.*PI))**2
      A4=MAB**2*(PI**2*(R2-R)**2+4.*(R2+R)**2)/(4.*PI**2)
      A5=A4*(G2**2*THETA(2)**4+(OMO+G1*THETA(2))**4)
      A6=A1-(MU*RH*G1)**2*A4/(1.+MU**2)
      A7=A2+2.*(MU*RH*THETA(2))**2*A4*G1*G2/(1.+MU**2)
      A8=A3-A5*(MU*RH)**2/(1.+MU**2)
      ARG=A7**2-4.*A6*A8
      IF(MU.LE.0.0)ARG=0.0
      DTHETA(2)=(A7+SQRT(ARG))/(2.*A6)
      RETURN
      END
```

```
      SUBROUTINE OUTP(TIME,THETA,DTHETA,IHLF,NDIM,PRMT)
      DIMENSION THETA(2),DTHETA(2),PRMT(5)
      COMMON DELTA,B,R10,R20,R0,E,RHOSP,RHOSH,M,L,OMO,RC,ALPHA,PI,I,
     1TURNMAX,MU,RH.RCM,IH
      REAL M,L,I,MU,MAB,IH
      ALPHA=-(R0+DELTA*THETA(1)/(4.*PI))*THETA(1)/(R20-R0-DELTA*THETA(1)
     1/(2.*PI))
      R=R0-DELTA*(ALPHA-THETA(1))/(2.*PI)
      R2=R20-DELTA*ABS(ALPHA)/(2.*PI)
      RAB=(R2+R)/2.
      M=E*B*R*(1.-R/R2)*(-DELTA+R*ALOG((2.*R+DELTA)/(2.*R-DELTA)))
      TURNS=-THETA(1)/(2.*PI)
      IF(TIME.EQ.0.0)J=0.0
      IF(J/50*50.NE.J)GO TO 2
      WRITE(6,1)TIME,TURNS,THETA(1),M,DTHETA(2),THETA(2),ALPHA
    2 J=J+1
    1 FORMAT(*OTIME=*,F5.3,3X,*TURNS=*,F6.2,3X,*THETA(1)=*,F7.2,3X,*M=*,
     1E12.4,3X,*THDOT=*,E12.6,3X,*THETA(2)=*,E12.6,3X,*ALPHA=*,F7.2)
      IF(TURNS.GE.TURNMAX.OR.THETA(2).GT.0.)PRMT(5)=1.
      RETURN
      END
```

```
DELTA= .003

B= .500

R10= .26

R20=1.00

E=   .30E+08

RHOSP=   .75E-03

RHOSH=   .75E-03

L= 71.9

OMO= 628.3

  MU=0.0000

IH=   .34E-05


TIME=0.000   TURNS=  0.00   THETA(1)=    0.00   M=   .5768E-01   THDOT=-.813590E+04   THETA(2)=0.              ALPHA=   0.00
TIME= .050   TURNS=  1.15   THETA(1)=   -7.21   M=   .5898E-01   THDOT=-.279932E+04   THETA(2)=-.245615E+03   ALPHA=   4.18
TIME= .100   TURNS=  3.51   THETA(1)= -22.06    M=   .6176E-01   THDOT=-.965513E+03   THETA(2)=-.333323E+03   ALPHA=  12.52
TIME= .150   TURNS=  6.29   THETA(1)= -39.51    M=   .6521E-01   THDOT=-.857338E+02   THETA(2)=-.357335E+03   ALPHA=  21.87
TIME= .200   TURNS=  9.11   THETA(1)= -57.25    M=   .6894E-01   THDOT= .412905E+03   THETA(2)=-.348076E+03   ALPHA=  30.92
TIME= .250   TURNS= 11.78   THETA(1)= -74.00    M=   .7270E-01   THDOT= .709114E+03   THETA(2)=-.319364E+03   ALPHA=  39.04
TIME= .300   TURNS= 14.16   THETA(1)= -89.00    M=   .7626E-01   THDOT= .868523E+03   THETA(2)=-.279427E+03   ALPHA=  45.98
TIME= .350   TURNS= 16.21   THETA(1)=-101.85    M=   .7949E-01   THDOT= .920263E+03   THETA(2)=-.234303E+03   ALPHA=  51.69
TIME= .400   TURNS= 17.89   THETA(1)=-112.42    M=   .8226E-01   THDOT= .886029E+03   THETA(2)=-.188836E+03   ALPHA=  56.22
TIME= .450   TURNS= 19.22   THETA(1)=-120.79    M=   .8454E-01   THDOT= .790742E+03   THETA(2)=-.146720E+03   ALPHA=  59.70
TIME= .500   TURNS= 20.24   THETA(1)=-127.19    M=   .8633E-01   THDOT= .662222E+03   THETA(2)=-.110314E+03   ALPHA=  62.30
TIME= .550   TURNS= 21.00   THETA(1)=-131.94    M=   .8770E-01   THDOT= .525808E+03   THETA(2)=-.806252E+02   ALPHA=  64.20
TIME= .600   TURNS= 21.54   THETA(1)=-135.37    M=   .8870E-01   THDOT= .399650E+03   THETA(2)=-.575577E+02   ALPHA=  65.55
TIME= .650   TURNS= 21.93   THETA(1)=-137.79    M=   .8941E-01   THDOT= .293362E+03   THETA(2)=-.403251E+02   ALPHA=  66.50
TIME= .700   TURNS= 22.20   THETA(1)=-139.48    M=   .8992E-01   THDOT= .209603E+03   THETA(2)=-.278437E+02   ALPHA=  67.16
TIME= .750   TURNS= 22.38   THETA(1)=-140.64    M=   .9026E-01   THDOT= .146728E+03   THETA(2)=-.190157E+02   ALPHA=  67.61
TIME= .800   TURNS= 22.51   THETA(1)=-141.42    M=   .9050E-01   THDOT= .101168E+03   THETA(2)=-.128821E+02   ALPHA=  67.91
TIME= .850   TURNS= 22.59   THETA(1)=-141.96    M=   .9066E-01   THDOT= .689915E+02   THETA(2)=-.867607E+01   ALPHA=  68.12
```

```
TIME= .900   TURNS= 22.65   THETA(1)=-142.31   M=   .9077E-01   THDOT= .466774E+02   THETA(2)=-.581903E+01   ALPHA=  68.25
TIME= .950   TURNS= 22.69   THETA(1)=-142.55   M=   .9084E-01   THDOT= .314048E+02   THETA(2)=-.389140E+01   ALPHA=  68.35
TIME=1.000   TURNS= 22.71   THETA(1)=-142.71   M=   .9089E-01   THDOT= .210457E+02   THETA(2)=-.259703E+01   ALPHA=  68.41
```

DISTRIBUTION LIST

Commander
U.S. Army Armament Resesarch
and Development Command
ATTN: DRDAR-TSS (5)
DRDAR-GCL
DRDAR-LCN (18)
DRDAR-LCA
Dover, NJ 07801

Administrator
Defense Technical Information Center
ATTN: Accessions Division (12)
Cameron Station
Alexandria, VA 22314

Director
U.S. Army Materiel Systems
Analysis Activity
ATTN: DRXSY-MP
Aberdeen Proving Ground, MD 21005

Commander/Director
Chemical Systems Laboratory
U.S. Army Armament Research
and Development Command
ATTN: DRDAR-CLJ-L
DRDAR-CLB-PA
APG, Edgewood Area, MD 21010

Director
Ballistic Research Laboratory
U.S. Army Armament Research
and Development Command
ATTN: DRDAR-TSB-S
Aberdeen Proving Ground, MD 21005

Chief
Benet Weapons Laboratory, LCWSL
U.S. Army Armament Research
and Development Command
ATTN: DRDAR-LCB-TL
Watervliet, NY 12189

Commander
U.S. Army Armament Materiel
Readiness Command
ATTN: DRSAR-LEP-L
Rock Island, Il 61299

Director
U.S. Army TRADOC Systems
  Analysis Activity
ATTN: ATAA-SL
White Sands Missile Range, NM 88002

Commander
Harry Diamond Laboratories
ATTN: Library
       DRSDO-DAB, D. Overman
2800 Powder Mill Road
Adelphi, MD 20783